Clays and Clay Minerals, Vol. 60, No. 3, 291–299, 2012.

p-NITROPHENOL ELECTRO-OXIDATION ON A BTMA$^+$-BENTONITE-MODIFIED ELECTRODE

A. Abu Rabi-Stanković*, A. Milutinović-Nikolić, N. Jović-Jovičić, P. Banković, M. Žunić, Z. Mojović, and D. Jovanović

University of Belgrade, Institute of Chemistry, Technology and Metallurgy, Department of Catalysis and Chemical Engineering, Njegoševa 12, 11000 Belgrade, Republic of Serbia

Abstract—Phenol and its derivatives are regarded as 'priority pollutants' and *p*-nitrophenol (*p*-NP), in particular, is of great interest due to its toxicity and frequent presence in waste waters and fresh waters. Straightforward, inexpensive methods to identify *p*-NP in water, however, is lacking. In the present study, an electrochemical technique using clay-modified electrodes to measure *p*-NP was investigated as a potentially promising method to fill that gap. A glassy carbon electrode (GCE) was modified with a thin layer of Na-enriched bentonite and a series of benzyltrimethylammonium (BTMA$^+$)-bentonites (BTMA$^+$-B) in order to confirm these materials as *p*-NP electrosensitive. A series of organobentonites was synthesized using different BTMA$^+$/bentonite ratios. The materials obtained were characterized using X-ray diffraction, Fourier-transform infrared spectroscopy, and a low-temperature nitrogen adsorption-desorption method. A monolayer arrangement of BTMA$^+$ within the interlamellar region of beidellite-rich smectite was confirmed. Deterioration of the textural properties was observed with increase of BTMA$^+$ loading. The electro-oxidation of *p*-NP in an acidic medium on BTMA$^+$-B-modified GCE was investigated. The cyclic voltammetry method with a three-electrode cell was used. The reference electrode was Ag/AgCl in 3 M KCl and a Pt foil was the counter electrode. For each electrochemical measurement, a different BTMA$^+$ loading in BTMA$^+$-B was used as the material for GCE coating and applied as the working electrode. The electrochemical activity of BTMA$^+$-B-based electrodes increased with BTMA$^+$ loading. The results confirmed that the organophylic character of the BTMA$^+$-B-modified surface was the main influence on the electrochemical activity of the BTMA$^+$-B-based GCE; the influence of textural properties was almost negligible. The increased electrode activity toward *p*-NP was achieved by the adsorption of *p*-NP on the electrode surface, the process that commonly precedes the electro-oxidation. The present study showed that synthesized materials could potentially be used in an electrochemical test for the presence of *p*-NP in water solutions.

Key Words—BTMA$^+$-bentonite, Cyclovoltammetry, Electrochemical Properties, Modified Electrode, Para-nitrophenol, Priority Pollutant.

INTRODUCTION

Aromatic nitrocompounds commonly used in the manufacture of explosives, pesticides, dyes, plasticizers, and pharmaceuticals are very toxic (Munnecke, 1976; Hallas and Alexander, 1983; Hanne *et al.*, 1993). These compounds have been detected not only in industrial wastewaters, but also in freshwater and in marine environments (Lypczynska-Kochany, 1992) and are regarded by the United States Environmental Protection Agency (USEPA) as 'priority pollutants,' due to the fact that they are toxic to humans (Lypczynska-Kochany, 1991). In particular, *p*-nitrophenol (*p*-NP) is a toxic derivative of the insecticide parathion which is also present in wastewaters from industries such as refineries.

An effective, straightforward, and inexpensive method for determining *p*-NP in water is essential. Various methods have been developed for the detection of *p*-NP and intermediates of *p*-NP degradation. Among them, liquid chromatography (LC) and gas chromatography-mass spectrometry (GC-MS) are commonly used (Oturan *et al*., 2000; Gao and Ren, 2010), though these techniques have poor detection limits. Electrochemical methods do not require sample pretreatment, are much simpler, and can be performed in opaque media, which makes them preferable to ultraviolet-visible (UV-Vis) spectrophotometry. To detect *p*-NP, electroanalytical techniques based on various chemically modified electrodes have been proposed (El Mhammedi *et al.*, 2009; Lupu *et al*., 2009; Alizadeh *et al*., 2009). Applications employing a microelectrode as the working electrode, *e.g.* a multiwall carbon nanotube (Moraes *et al.*, 2009), nanoporous gold (Liu *et al*., 2009), and zirconia (Liu and Lin, 2005), have been reported recently. Clay-modified electrodes have received attention because clays are inexpensive materials which are modified easily and have the ability to preconcentrate analytes, leading to greater sensitivity and lower detection limits (Fitch, 1996).

Exchangeable cations residing in the interlayers of the smectites in bentonite can be replaced by organic

* E-mail address of corresponding author:
andjela.aburabi@gmail.com
DOI: 10.1346/CCMN.2012.0600306

cations such as alkylammonium ions *via* an ion-exchange reaction to render layered silicates organophilic (Lagaly *et al*., 2006; Uslu *et al*., 2009). As a result, organoclays are excellent adsorbents for the removal of phenolic compounds (Shen, 2002; Al-Asheh *et al.*, 2003; Senturk *et al.*, 2009). Organoclays can also be used as electrode materials for electrochemical determination (Hu *et al*., 2001; Yang *et al*., 2008) or electrochemical degradation (Iurascu *et al*., 2009; Ma *et al*., 2009) of phenolic compounds. Aromatic organoclays as electrode materials have attracted a lot of attention; however, this research area has not been investigated fully. Due to the fact that *p*-NP is an aromatic compound, the main assumption was that a benzyltrimethylammonium-bentonite ($BTMA^+$-B)-based electrode would be a *p*-NP electrosensitive material. The present study reports the results of the synthesis and characterization of a series of $BTMA^+$-B rich in beidelite. The influence of $BTMA^+$ loading on the properties of the materials obtained was investigated to correlate structural and textural properties with electrochemical behavior. The electrochemical investigation was performed on a GCE modified by the synthesized $BTMA^+$-bentonites. The $BTMA^+$-modified GCEs were tested for the electro-oxidation of *p*-NP. Multisweep cyclic voltammetry was used in order to investigate the effect of surfactant loading on the electrochemical behavior of the modified electrodes. The aim was to test these materials as possible sensors for *p*-NP detection in waste waters and in fresh waters.

EXPERIMENTAL

Materials

Bentonite was obtained from Bogovina Coal and Bentonite Mine, Serbia. It was crushed, ground, and sieved through a 74 μm sieve (19.5 cm diameter stainless steel sieve from Fosil, Arilje, Serbia). The chemical composition (wt.%) of the raw clay (<74 μm) and the particle-size distribution were reported previously (Vuković *et al.*, 2006; Krstić *et al.*, 2011).

Benzyltrimethylammonium ($BTMA^+$) bromide was obtained from Alfa-Aesar Chemical Company (Karlsruhe, Germany) with a purity of 98% and used as received.

Preparation of $BTMA^+$-bentonites

The first step was Na^+-modification of the raw bentonite material (particle size up to 74 μm) to obtain homoionic clay (Na^+-bentonite) by means of a commonly used procedure (Jović-Jovičić *et al.*, 2008; Carrado *et al.*, 2006). The cation exchange capacity (CEC) of Na^+-bentonite (Na^+-B) was determined by the standard ammonium acetate method (Environmental Protection Agency, 1986; Bergaya *et al.*, 2006). The CEC of the bentonite was 0.633 meq/g. A standard procedure for preparing organo-bentonite was used (Jović-Jovičić *et al.*, 2010). A volume of 100 mL of $BTMA^+$ solution was added to a stirred Na^+-B dispersion. The series of organo-bentonites with different $BTMA^+$/bentonite ratios (0.127, 0.317, 0.633, and 1.266 mmol/g) was synthesized. After stirring for 24 h, the dispersion was filtered through a Buchner funnel (Filtrak 388 filter paper was used). The filtration cake was washed with distilled water until the bromide test with 0.1 M $AgNO_3$ was negative. The amount of $BTMA^+$ cations was expressed in multiples of the CEC with values of 0.2, 0.5, 1.0, and 2.0; the samples were denoted as 0.2 $BTMA^+$-B, 0.5 $BTMA^+$-B, 1.0 $BTMA^+$-B, and 2.0 $BTMA^+$-B.

Methods

The $BTMA^+$-bentonite sample analyses were checked for their carbon, hydrogen, and nitrogen contents using a Vario EL III device (Hanau Instruments GmbH, Germany). Elemental analysis was calculated from multiple determinations within ±0.2% agreement.

The X-ray diffraction (XRD) patterns of the powders of Na^+-B and the series of $BTMA^+$-B were obtained using a Philips PW 1710 X-ray powder diffractometer (Philips, Eindhoven and Almelo, The Netherlands) with a Cu anode (λ = 0.154178 nm).

The FTIR spectra of the Na^+-B and different $BTMA^+$-B samples were obtained using a Thermo Nicolet 6700 FT-IR Spectrophotometer (Allschwil, Switzerland). The KBr pressed-disc technique (2 mg of sample and 200 mg of KBr) was used.

Nitrogen adsorption-desorption isotherms were determined using a Sorptomatic 1990, Thermo Finnigan device (Allschwil, Switzerland) at −196ºC. The samples were outgassed at 80ºC for a period of 10 h. The specific surface area of the samples, S_{BET}, was calculated according to the Brunauer, Emmett, Teller (BET) method (Gregg and Sing, 1967; Rouquerol *et al.*, 1999) from the linear parts of the nitrogen adsorption isotherms. The total pore volume was calculated according to the Gurvitch method for p/p_0 = 0.98 (Gregg and Sing, 1967; Rouquerol *et al.*, 1999). The volume of mesopores was calculated according to the Barrett, Joyner, Halenda (BJH) method from the desorption branch of the isotherm (Webb and Orr, 1997). Micropores were analyzed using the Dubinin-Radushkevich method (Dubinin, 1975).

In order to use the modified bentonites as electrode materials, the organo-bentonite samples were dispersed homogeneously in a 5 wt.% Nafion solution in a mixture of isopropyl alcohol and water using an ultrasonic bath. The electrical conductivity of the sample was enhanced by adding 10 wt.% of carbon black Vulcan XC72 (Cabot Corporation, Boston, Massachusetts, USA) to the initial dispersion. A droplet of each dispersion was placed on the surface of a glassy carbon rotating-disc electrode. After removal of the solvent by evaporation at 90ºC, modified bentonite particles were distributed uniformly on the glassy carbon support in the form of a thin layer and used as the working electrode.

For the electrochemical investigations, a three-electrode, all-glass cell was employed. A prepared $BTMA^+$-B-modified GCE was used as the working electrode. The reference electrode was Ag/AgCl in 3 M KCl and Pt foil was the counter electrode. The electrochemical measurements were made using a 757 VA Computrace instrument from Metrohm (Herisau, Switzerland). The cyclic voltammograms (CV) were recorded at the potential scan rate of 10 mV s^{-1}. The $BTMA^+$-B-based electrodes were investigated in 0.1 M H_2SO_4 solution.

RESULTS AND DISCUSSION

Sample characterization

The C, H, and N contents in the $BTMA^+$-bentonites obtained were analyzed (Table 1). The theoretical values of the elements were also calculated according to the CEC value.

The difference between calculated and experimental values was very small, which confirmed that the amount of BTMA+ cations loaded was in agreement with the amounts introduced. The amounts of C, H, and N increased with the $BTMA^+$ loading.

The XRD patterns of the Na^+-B and of the different $BTMA^+$-B samples (Figure 1) revealed that the Na^+-B consisted mainly of smectite in admixtures with quartz (MacEwan and Wilson, 1980; International Center for Diffraction Data, 1990).

Incorporation of $BTMA^+$ led to an increase in the d_{001} smectite basal spacing, from 1.38 to 1.46 nm. The d_{001} basal spacing values obtained for all $BTMA^+$-B samples corresponded to the monolayer arrangements of $BTMA^+$ between the smectite layers (Lagaly *et al.*, 2006).

The FTIR spectra of the Na^+-B and 2.0 $BTMA^+$-B are reported (Figure 2), including an expanded scale for the regions of particular interest for sample 2.0 BTMA-B (Figures 2a and 2b). The spectra of $BTMA^+$-B with lower loadings were omitted because spectral responses were rather weak, even for the greatest $BTMA^+$ loading.

Table 1. Analyses of the $BTMA^+$-bentonites.

Sample	C (wt.%)	H (wt.%)	N (wt.%)
Calculated values			
0.2 BTMA-B	1.49	0.20	0.17
0.5 BTMA-B	3.62	0.48	0.42
1.0 BTMA-B	6.94	0.93	0.81
2.0 BTMA-B	12.77	1.70	1.49
Experimental values			
0.2 BTMA-B	1.51	0.22	0.15
0.5 BTMA-B	3.42	0.42	0.41
1.0 BTMA-B	6.81	0.95	0.77
2.0 BTMA-B	12.55	1.64	1.45

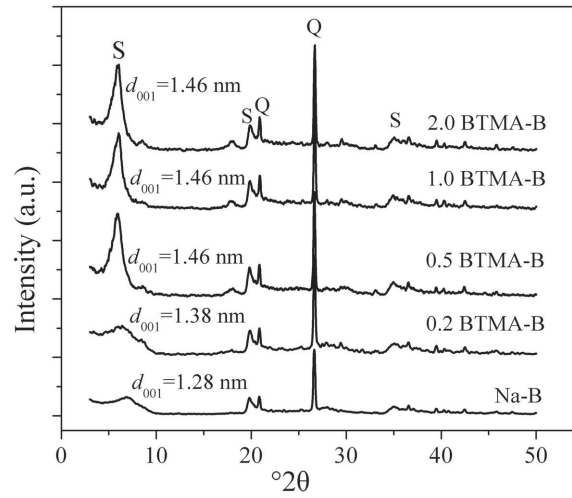

Figure 1. XRD traces of the Na^+-B and of various $BTMA^+$-B samples (S = smectite, Q = quartz).

In the Na^+-B spectra, all observed bands were assigned to smectite (Table 2) (Madejová *et al.*, 1994, 1998; Komadel *et al.*, 1996; Breen and Watson, 1998; Falaras *et al.*, 1999; Majumdar *et al.*, 2003) other than those assigned to calcite and quartz.

The FTIR spectrum of 2.0 $BTMA^+$-B (Figures 2a, 2b, Table 2) consisted of absorption bands characteristic of bentonite and the $BTMA^+$ cation. All the bands of bentonite origin were also observed in the 2.0 $BTMA^+$-B spectrum. The bands related to the $BTMA^+$ cation were

Table 2. Characteristic bands of Na^+-B and 2.0 $BTMA^+$-B.

Vibrations	Wavenumber (cm^{-1})
Smectite	
Quartz	799
Calcite	1430
ν_sOH in smectites (AlFe, FeMg, FeFe)	3587–3532
ν_sOH in smectite (AlAl and AlMg)	3684–3604
ν_sOH– (from interlayer water)	3420
δ_sOH– (from interlayer water)	
ν_sSi–O–Si	1045
δ_sSi–O–Si	690
δ_sOH– in AlAlOH	920
δ_sOH– in AlFeOH	860
2.0 $BTMA^+$–B	
$\nu_{as}CH_3$–N	3034
$\nu_s CH_3$–N	2960
$\nu_{as}CH_2$	2926
$\nu_s CH_2$	2854
νCH (Ar)	3068
ν_{as}C–C(Ar)	1495, 1486
$\delta_{as}CH_2$	1466
$\delta_s CH_2$	1425
$\delta_s CH_3$	1377
δ_{opp} C–H(Ar)	727

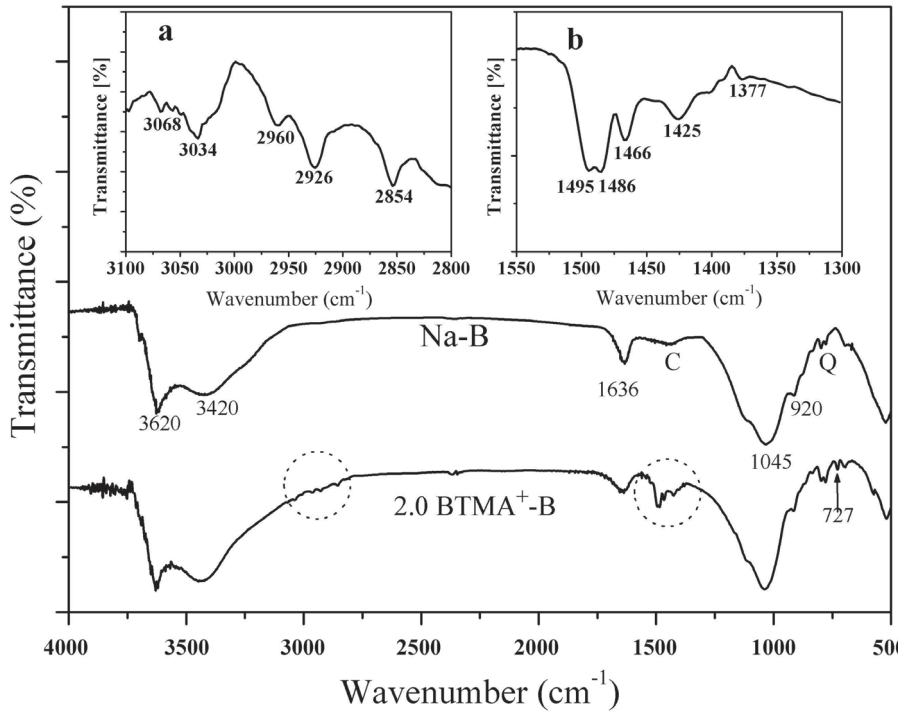

Figure 2. FTIR spectra of Na^+-B and 2$BTMA^+$-B (the FTIR spectra of 2.0 $BTMA^+$-B in the 3100−2800 cm^{-1} and 1550−1300 cm^{-1} regions are embedded in parts a and b, respectively).

also present in the 2.0 $BTMA^+$-B spectrum, though less pronounced. The intensities of the CH bands corresponding to aromatic cations were lower than those corresponding to aliphatic cations (Jankovič *et al.*, 2011). The interpretation of the 3100−3000 cm^{-1} region was more complicated due to the possible overlap of different vibrational modes (Falaras *et al.*, 1999). The stretching modes of CH bonds in the benzene ring, νCH(Ar), overlapped frequently in this region. The low-intensity band at 3068 cm^{-1}, therefore, probably corresponded to νCH (Ar). The band at 727 cm^{-1} in $BTMA^+$-B spectra arose from δ_{opp} C-H(Ar). This band indicated the presence of five H atoms in a benzene ring, which implies that it corresponds to a monosubstituted benzene derivative (Pretsch *et al.*, 1981). The FTIR spectra confirmed the presence of $BTMA^+$ in smectite.

The nitrogen adsorption-desorption isotherms of the Na^+-B and the $BTMA^+$-B with different $BTMA^+$ loadings (Figure 3) revealed that the adsorption isotherms for all samples investigated belong to the Type II isotherms according to the IUPAC classification. A large uptake of nitrogen was observed close to the saturation pressure, indicating multilayer adsorption and implying the presence of mesopores (Wang *et al.*, 2004).

Textural properties calculated from the adsorption isotherm data for all the samples investigated (Table 3) revealed that the specific mesopore and micropore surface areas (S_{BET} and S_{mic}, respectively) of the Na^+-B/$BTMA^+$-bentonites decreased as the amount of $BTMA^+$ increased. The intercalation of $BTMA^+$ into smectite layers led to decreases in the total, meso-, and micropore volumes. Increasing the surfactant loading led to deterioration of the textural properties caused by increased partial pore blockage that inhibited the passage of nitrogen molecules.

Electrochemical investigations

Based on a previous investigation of phenol electrooxidation on aluminosilicate-based electrodes in different media, a well pronounced signal was obtained in acidic electrolytes (Mojović *et al.*, 2011). The electro-

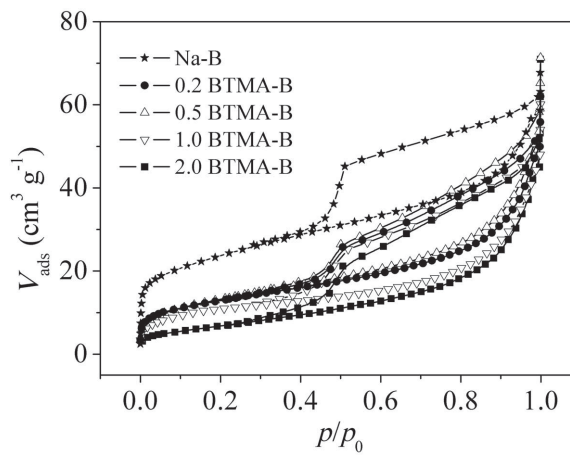

Figure 3. N_2 adsorption-desorption isotherms of Na^+-B and $BTMA^+$-B for different $BTMA^+$ loadings.

Table 3. Textural properties of Na-B and different $BTMA^+$-B samples.

Sample	$V_{0.98}$ ($cm^3\ g^{-1}$)	V_{meso} ($cm^3\ g^{-1}$)	V_{mic} ($cm^3\ g^{-1}$)	D_{med} (nm)	D_{max} (nm)	S_{BET} ($m^2\ g^{-1}$)	S_{mic} ($m^2\ g^{-1}$)
Na-B	0.088	0.0837	0.0331	3.94	3.86	84	93
0.2 $BTMA^+$	0.077	0.0776	0.0191	5.02	3.96	50	54
0.5 $BTMA^+$	0.075	0.0768	0.0185	5.53	3.93	48	52
1.0 $BTMA^+$	0.071	0.0753	0.0176	5.46	3.91	46	50
2.0 $BTMA^+$	0.065	0.0729	0.0146	4.99	3.84	39	41

Where: $V_{0.98}$ = total pore volume, V_{meso} = volume of mesopores, V_{mic} = volume of micropores, D_{med} = median mesopore diameter, D_{max} = the most abundant mesopore diameter, S_{BET} = specific surface area, S_{mic} = specific micropore surface.

chemical behavior of the $BTMA^+$-B-based electrodes in *p*-NP was, therefore, investigated in 0.1 M H_2SO_4 as a supporting electrolyte.

The electrochemical behavior of the Na^+-B and $BTMA^+$-B-modified electrodes in 0.1 M H_2SO_4 (Figure 4) was studied over a wide range of potential, from hydrogen evolution at ~−0.3 V to oxygen evolution at ~1.4 V.

All of the electrodes investigated deteriorated during cycling (Figure 4). The most significant change in all cases was noted between the first and second cycles with respect to the peak at ~1.0 V. This peak decreased rapidly with cycling and became insignificant at steady state. The pair of peaks at ~0.5 V, the height of which increased with cycling, was attributed to the oxidation/reduction of the Fe^{2+}/Fe^{3+} redox couple (Banković *et al.*, 2010). Bearing in mind the large percentage of Fe in the Na^+-B (Vuković *et al.*, 2006), this oxidation/reduction process could reasonably be expected to occur on every bentonite-based electrode, because organomodification does not reduce Fe content.

The currents obtained for all of the electrodes investigated were of the same order of magnitude, but clear evidence of the current-density change caused by $BTMA^+$ loading was absent.

After five cycles, when the steady state had been reached, cycling was continued at the same rate up to ten cycles in 10 mM *p*-NP +0.1 M H_2SO_4 solution (Figure 5).

In 10 mM *p*-NP+0.1 M H_2SO_4, the peak at ~1.0 V assigned to *p*-NP was registered for all investigated electrodes (Figure 5). This peak decreased significantly

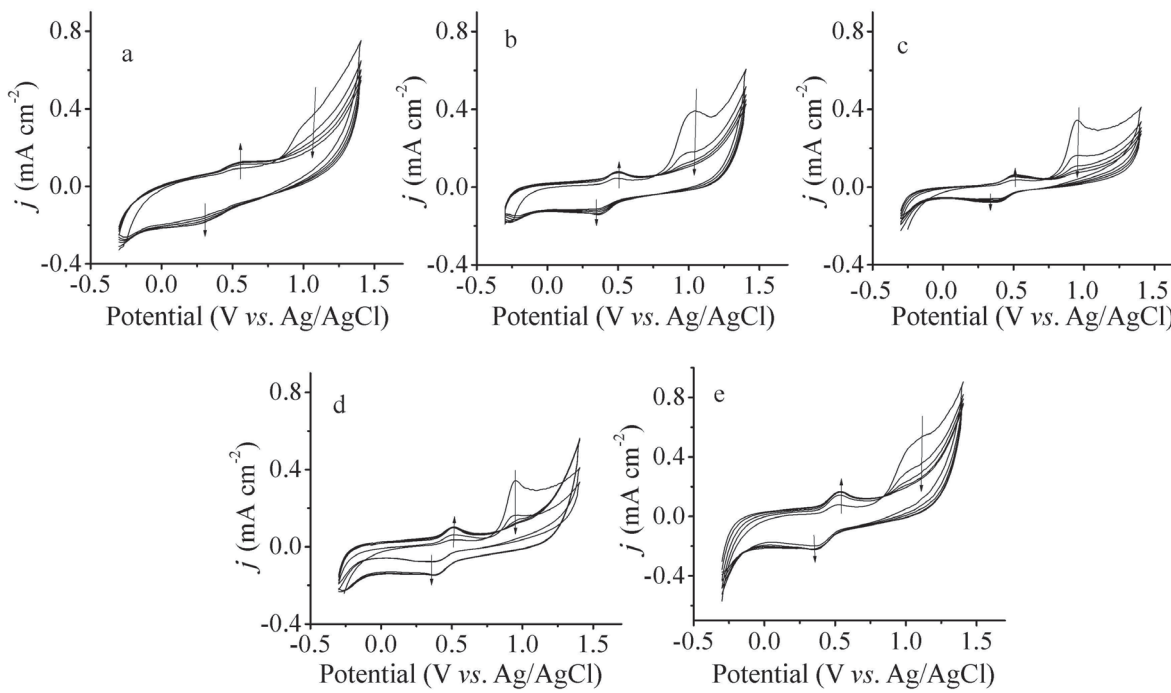

Figure 4. Cyclic voltammograms of bentonite-based electrodes in 0.1 M H_2SO_4: (a) Na^+-B; (b) 0.2 $BTMA^+$-B; (c) 0.5 $BTMA^+$-B; (d) 1.0 $BTMA^+$-B; and (e) 2.0 $BTMA^+$-B. The scan rate was 10 mV s^{-1}. Arrows indicate changes during cycling.

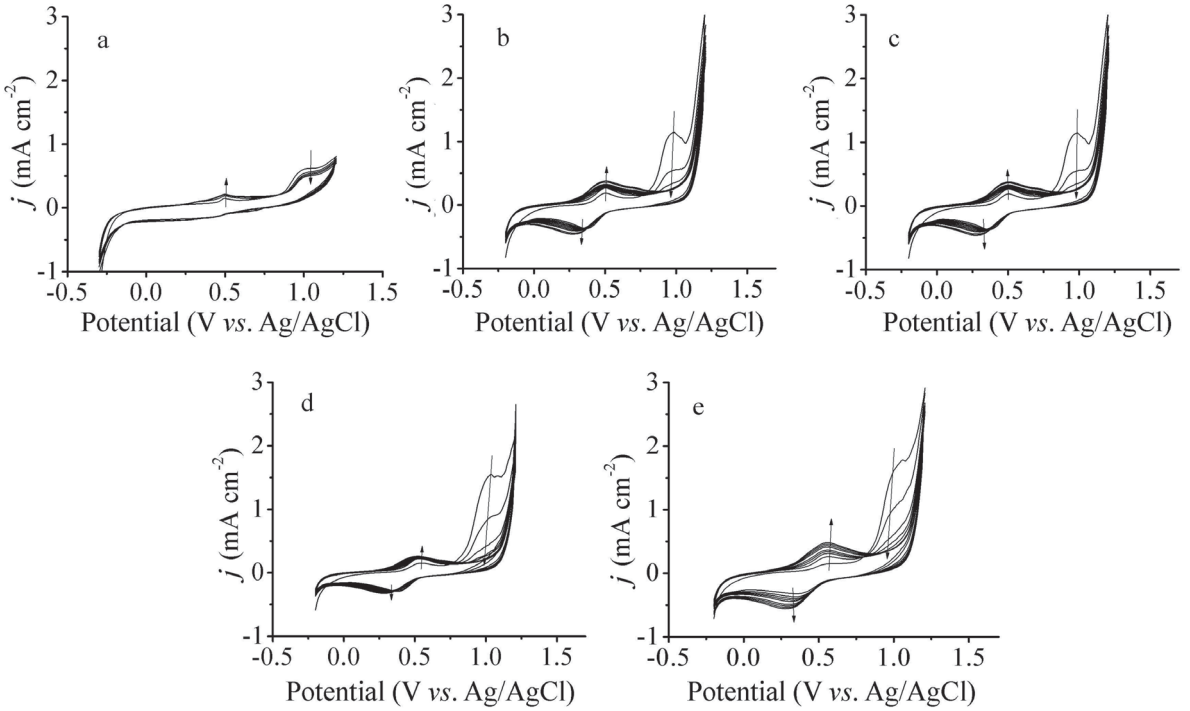

Figure 5. Cyclic voltammograms of bentonite-based electrodes in 10 mM *p*-NP+0.1 M H_2SO_4: (a) Na^+-B; (b) 0.2 $BTMA^+$-B; (c) 0.5 $BTMA^+$-B; (d) 1.0 $BTMA^+$-B; and (e) 2.0 $BTMA^+$-B. The scan rate was 10 mV s^{-1}. Arrows indicate changes during cycling.

during cycling. A similar phenomenon was observed when HDTMA-based electrodes were used in phenol electro-oxidation (Mojović *et al.*, 2011). During the *p*-NP oxidation, a series of products was obtained, reflected in the appearance of broad waves at ~0.5 V. According to Oturan *et al.* (2000), major intermediary degradation products of *p*-NP such as hydroquinone, benzoquinone, 4-nitrocatechol, 1,2,4-trihydroxybenzene, and 3,4,5-trihydroxy-nitrobenzene were identified unequivocally by high-performance LC and GC-MS methods. Electrochemical methods were used (Safavi *et al.*, 2007) to confirm the occurrence of *p*-benzoquinone and hydroquinone and the peaks registered at 0.47 V and 0.64 V were assigned to these compounds, respectively. The current density of these peaks increased during cycling (Figure 5). The same shape for the cyclic voltammograms of all the electrodes investigated indicated the existence of identical oxidation-reduction processes. The electrodes differed only in terms of the current density of corresponding peaks (Figure 6).

The current density for the *p*-NP oxidation wave at ~1.0 V increased in the following order: Na^+-B < 0.2 $BTMA^+$-B < 0.5 $BTMA^+$-B < 1 $BTMA^+$-B < 2 $BTMA^+$-B (Figure 6).

Although the textural properties of the samples decreased with increasing $BTMA^+$ loading, the activity of the electrode toward *p*-NP showed the opposite trend. The behavior observed suggested that the textural properties did not have a dominant role in the electro-oxidation process. The increased electrode activity toward *p*-NP can be assumed to have been due to the adsorption of *p*-NP on the electrode surface, because adsorption commonly precedes the electro-oxidation process. Data from the literature indicate that the adsorption of organic compounds increased with increasing organophilicity of the adsorbents regardless of the decrease in S_{BET} (Özcan *et al.*, 2005; Vuković *et al.*, 2006).

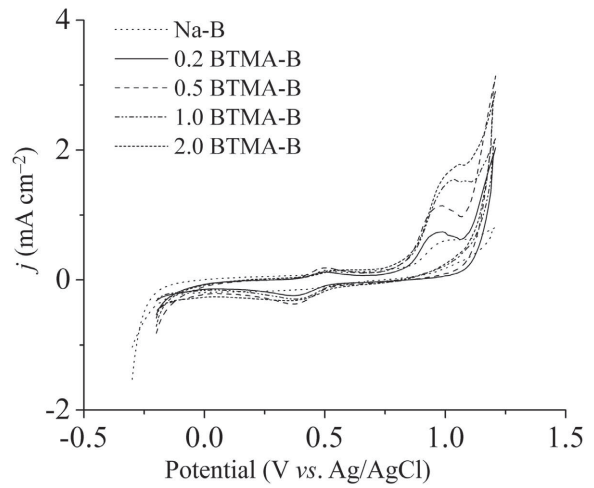

Figure 6. Cyclic voltammograms of bentonite-based electrodes in 10 mM *p*-NP+0.1 M H_2SO_4 (the first cycles): (a) Na^+-B; (b) 0.2 $BTMA^+$-B; (c) 0.5 $BTMA^+$-B; (d) 1.0 $BTMA^+$-B; and (e) 2.0 $BTMA^+$-B.

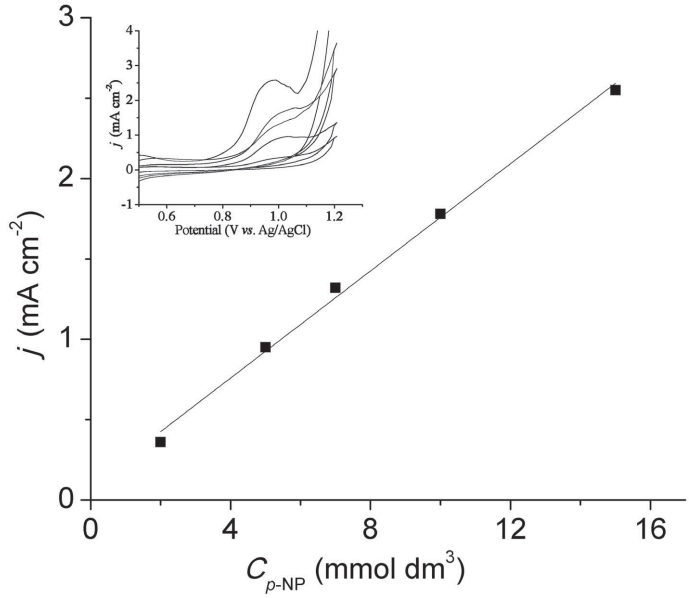

Figure 7. Anodic peak current density at potential ~1.0 V *vs*. *p*-NP concentration. Embedded: cyclic voltammograms for 2.0 $BTMA^+$-B for different $C_{p\text{-NP}}$ (the concentrations presented from bottom to top are 2−15 mmol dm^{-3}).

In a further investigation, the influence of *p*-NP concentration on the current density of the anodic peak at *E* ~1.0 V was studied using a 2.0 $BTMA^+$-B based electrode (as 2.0 $BTMA^+$-B has shown the best electrochemical response for *p*-NP oxidation) at a polarization rate of 10 mV s^{-1} (Figure 7). Due to previously observed electrode deactivation with aging, a freshly prepared electrode was used for each experiment. The current density, *j*, of the first anodic peak varied linearly (Equation 1) with the *p*-NP concentration, $C_{p\text{-}NP}$, with a coefficient of correlation (R) of 0.995, *viz.*

$$j = 0.092 + 0.167C_{p\text{-NP}} \quad (1)$$

The oxidation reaction of *p*-NP at different scan rates in the range 5−100 mV s^{-1} was also investigated. The results (Figure 8) revealed that the logarithm of current density (*j*) varied linearly with the logarithm of scan rate (ν).

The slope obtained was ~0.7, indicating a combined adsorption/diffusion-controlled process (Laviron, 1979).

CONCLUSIONS

A series of benzyltrimethylammonium ($BTMA^+$) bentonites with different $BTMA^+$/bentonite ratios was

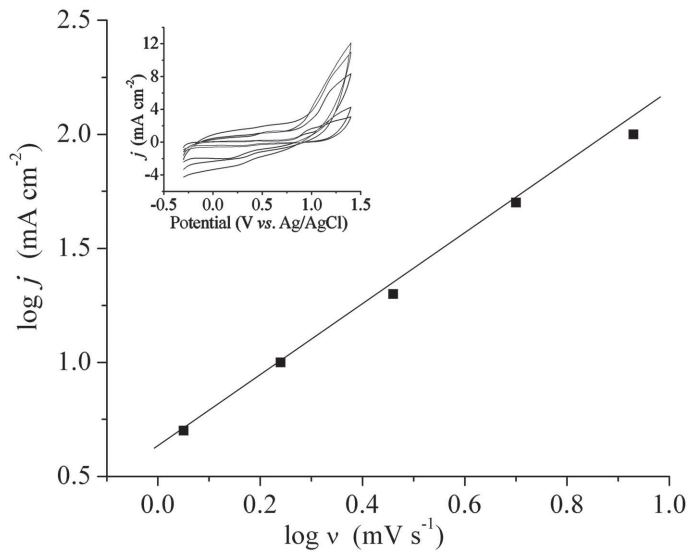

Figure 8. The dependence of log *j* on log ν. Embedded: cyclic voltammograms for 2.0 $BTMA^+$-B in 10 mM *p*-NP + 0.1 M H_2SO_4 at different scan rates (the scan rates presented from bottom to top are 5−100 mV s^{-1}).

prepared using bentonite from a local deposit in Serbia. The samples obtained were characterized using XRD, FTIR, and the nitrogen physisorption method. The incorporation of $BTMA^+$ led to an increase in the smectite d_{001} basal spacing from 1.38 to 1.46 nm indicating monolayer arrangements of $BTMA^+$ intercalated into the smectite. The FTIR absorption bands of $BTMA^+$-B related to smectite and quartz remained unaffected by the incorporation of $BTMA^+$. In addition, the bands assigned to the ν and δ vibrations characteristic of the $BTMA^+$ cation were registered and identified. Textural properties deteriorated with increasing $BTMA^+$ loading. The electrochemical properties of the $BTMA^+$-B-based electrodes in the electro-oxidation of *p*-NP were investigated and the electrochemical activity of $BTMA^+$-B-based electrodes increased with $BTMA^+$ loading. Keeping in mind that adsorption commonly precedes electro-oxidation, the increased electrode activity toward *p*-NP was presumably achieved because the more organophilic electrode surface favored *p*-NP adsorption. For the 2.0 $BTMA^+$-B-based electrode, the current density showed a linear dependence on the concentration of *p*-NP. In addition, the logarithm of current density showed linear dependence on the logarithm of scan rate, indicating that synthetic materials could potentially be used for electrochemical testing for the presence of *p*-NP in aqueous solutions.

ACKNOWLEDGMENTS

The present study work was supported by the Ministry of Education and Science of the Republic of Serbia (Project III 45001).

REFERENCES

Al-Asheh, S., Banat, F., and Abu-Aitah, L. (2003) Adsorption of phenol using different types of activated bentonites. *Separation and Purification Technology*, **33**, 1–10.

Alizadeh, T., Ganiali, M.R., Norouzi, P., Zare, M., and Zeraatkar, A. (2009) A novel high selective and sensitive para-nitrophenol voltammetric sensor, based on a molecularly imprinted polymer-carbon paste electrode. *Talanta*, **79**, 1197–1203.

Banković, P., Mojović, Z., Milutinović-Nikolić, A., Jović-Jovičić, N., Marinović, S., and Jovanović, D. (2010) Mixed pillared bentonite for electrooxidation of phenol. *Applied Clay Science*, **49**, 84–89.

Bergaya, F., Lagaly, G., and Vayer, M. (2006) Cation and anion exchange. Pp. 979–1002 in: *Handbook of Clay Science* (F. Bergaya, B.K.G. Theng, and G. Lagaly, editors). Elsevier, Amsterdam.

Breen, C. and Watson, R. (1998) Acid-activated organoclays: preparation, characterisation and catalytic activity of polycation-treated bentonites. *Applied Clay Science*, **12**, 479–494.

Carrado, K.A., Decarreau, A., Petit, S., Bergaya, F., and Lagaly, G. (2006) Synthetic clay minerals and purification of natural clays. Pp. 115–140 in: *Handbook of Clay Science* (F. Bergaya, B.K.G. Theng, and G. Lagaly, editors). Elsevier, Amsterdam.

Dubinin, M.M. (1975) *Progress in Surface and Membrane Science*. Academic Press, New York.

El Mhammedi, M.A., Achak, M., Bakasse, M., and Chtaini, A. (2009) Electrochemical determination of para-nitrophenol at apatite-modified carbon paste electrode: Application in river water samples. *Journal of Hazardous Materials*, **163**, 323–328.

Environmental Protection Agency (1986) Method 9080 – Cation exchange capacity of soils (ammonium acetate). http://www.epa.gov/wastes/hazard/testmethods/sw846/pdfs/9080.pdf

Falaras, P., Kovanis, I., Lezou, F., and Seiragakis, G. (1999) Cottonseed oil bleaching by acid-activated montmorillonite. *Clay Minerals*, **34**, 221–232.

Fitch, A. (1996) Clay modified electrodes; a review. *Clays and Clay Minerals*, **38**, 391–400.

Gao, L. and Ren, S. (2010) Prediction of nitrophenol-type compounds using chemometrics and spectrophotometry. *Analytical Biochemistry*, **405**, 184–191.

Gregg, S.H. and Sing, K.S. (1967) *Adsorption, Surface Area and Porosity.* Academic Press, New York.

Hallas, L.E. and Alexander, M. (1983) Microbial transformation of nitroaromatic compounds in sewage effluent. *Applied and Environmental Microbiology*, **5**, 1234–1241.

Hanne, L.F., Kirk, L.L., Appel, S.M., Narayan, A.D., and Bains, K.K. (1993) Degradation and induction specicity in actinomycetes that degrade p-nitrophenol. *Applied and Environmental Microbiology*, **9**, 3505–3508.

Hu, S., Xu, C., Wang, G., and Cui, D. (2001) Voltammetric determination of 4-nitrophenol at a sodium montmorillonite-anthraquinone chemically modified glassy carbon electrode. *Talanta*, **54**, 115–123.

International Centre for Diffraction Data – Joint Committee on Powder Diffraction Standards, Powder diffraction data, Swarthmore, PA, USA (1990).

Iurascua, B., Siminiceanua, I., Vioneb, D., Vicentec, M.A., and Gil, A. (2009) Phenol degradation in water through a heterogeneous photo-Fenton process catalyzed by Fe-treated laponite. *Water Research*, **43**, 1313–1322.

Jankovič, L'., Madejová, J., Komadel, P., Jochec-Mošková, D., and Chodák, I. (2011) Characterization of systematically selected organo-montmorillonites for polymer nano composites. *Applied Clay Science*, **51**, 438–444.

Jović-Jovičić, N., Milutinović-Nikolić, A., Gržetić, I., and Jovanović, D. (2008) Organobentonite as efficient textile dye sorbent. *Chemical Engineering & Technology*, **31**, 567–574.

Jović-Jovičić, N., Milutinović-Nikolić, A., Banković, P., Mojović, Z., Žunić, M., Gržetić, I., and Jovanović, D. (2010) Organo-inorganic bentonite for simultaneous adsorption of acid orange 10 and lead ions. *Applied Clay Science*, **47**, 452–456.

Komadel, P., Bujdák, J., Madejová, J., Šucha, V., and Elsass, F. (1996) Effect of non-swelling layers on the dissolution of reduced-charge montmorillonite with various Li contents. *Clay Minerals*, **31**, 333–345.

Krstić, J., Mojović, Z., Abu Rabi, A., Lončarević, D., Vukelić, N., and Jovanović, D. (2011) Adsorption of methylene blue from aqueous solution onto bentonite. Pp. 1097–1106 in: *Survival and Sustainability: Environmental Concerns in the 21st Century* (H. Gökçekuş, U. Türker, and J.W. LaMoreaux, editors). Springer, Berlin.

Lagaly, G., Ogawa, M., and Dekany, I. (2006) Developments in clay science. Pp. 327–330 in: *Handbook of Clay Science* (F. Bergaya, B.K.G. Theng, and G. Lagaly, editors). Elsevier, Amsterdam.

Laviron, E. (1979) General expression of the linear potential sweep voltammogram in the case of diffusionless electrochemical systems. *Journal of Electroanalytical Chemistry*, **101**, 19–28.

Liu, G. and Lin, Y. (2005) Electrochemical sensor for

organophosphate pesticides and nerve agents using zirconia nanoparticles as selective sorbents. *Analytical Chemistry*, **77**, 5894–5901.

Liu, Z., Du, J., Qiu, C., Huang, L., Ma, H., Shen, D., and Ding, Y. (2009) Electrochemical sensor for detection of p-nitrophenol based on nanoporous gold. *Electrochemistry Communications*, **11**, 1365–1368.

Lupu, S., Lete, C., Marin, M., Totir, N., and Balaure, P.C. (2009) Electrochemical sensors based on platinum electrodes modified with hybrid inorganic-organic coatings for determination of 4-nitrophenol and dopamine. *Electrochimica Acta*, **54**, 1932–1938.

Lypczynska-Kochany, E. (1991) Degradation of aqueous nitrophenols and nitrobenzene by means of the Fenton reaction. *Chemosphere*, **22**, 529–536.

Lypczynska-Kochany, E.J. (1992) Degradation of nitrobenzene and nitrophenols in homogeneous aqueous solution. Direct photolysis versus photolysis in the presence of hydrogen peroxide and the Fenton reagent. *Water Pollutant Research Journal of Canada*, **27**, 97–122.

Ma, H., Zhang, X., Mab, Q., and Wang, B. (2009) Electrochemical catalytic treatment of phenol wastewater. *Journal of Hazardous Materials*, **165**, 475–480.

MacEwan, D.M.C. and Wilson, M.J. (1980) Interlayer and intercalation complexes of clay minerals. Pp. 197–248 in: *Crystal Structures of Clay Minerals and their X-ray Identification* (G.W Brindley and G. Brown, editors). Monograph **5**, Mineralogical Society, London.

Majumdar, D., Blanton, T.N., and Schwark, D.W. (2003) Clay-polymer nanocomposite coatings for imaging application. *Applied Clay Science*, **23**, 265–273.

Madejová, J., Komadel, P., and Čičel, B. (1994) Infrared study of octahedral site populations in smectites. *Clay Minerals*, **29**, 319–326.

Madejová, J., Bujdak, J., Janek, M., and Komadel, P. (1998) Comparative FT-IR study of structure modifications during acid treatment of dioctahedral smectites and hectorite. *Spectrochimica Acta A*, **54**, 1397–1406.

Mojović, Z., Jović-Jovičić, N., Banković, P., Žunić, M., Abu Rabi-Stanković, A., Milutinović-Nikolić, A., and Jovanović, D. (2011) Electrooxidation of phenol on different organo bentonite-based electrodes. *Applied Clay Science*, **53**, 331–335.

Moraes, F.C., Tanimoto, S.T., Salazar-Band, G.R., Machado, S.A.S., and Mascaro, L.H. (2009) A new indirect electroanalytical method to monitor the contamination of natural waters with 4-nitrophenol using multiwall carbon nanotubes. *Electroanalysis*, **21**, 1091–1098.

Munnecke, D.M. (1976) Enzymatic hydrolysis of organophosphate insecticides, a possible pesticide disposal method. *Applied and Environmental Microbiology*, **32**, 7–13.

Oturan, M.A., Peiroten, J., Chartrin, P., and Acher, A.J. (2000) Complete destruction of p-nitrophenol in aqueous medium by electro-Fenton method. *Environmental Science & Technology*, **34**, 3474–3479.

Özcan, A.S., Erdem, B., and Özcan, A. (2005) Adsorption of Acid Blue 193 from aqueous solutions onto BTMA-bentonite. *Colloids and Surfaces A*, **266**, 73–81.

Pretsch, E., Seibl, J., and Simon, W. (1981) *Tabellen zur strukturafklärung organischer verbindungen mit spektroskopischen methoden.* Springer Verlag, Berlin, Heidelberg.

Rouquerol, F., Rouquerol, J., and Sing, K. (1999) *Adsorption by Powders and Porous Solids*. Academic Press, London.

Safavi, A., Maleki, N., and Tajabadi, F. (2007) Highly stable electrochemical oxidation of phenolic compounds at carbon ionic liquid electrode. *The Analyst*, **132**, 54–58.

Senturk, H.B., Ozdes, D., Gundogdu, A., Duran, C., and Soylak M. (2009) Removal of phenol from aqueous solutions by adsorption onto organomodified Tirebolu bentonite: Equilibrium, kinetic and thermodynamic study. *Journal of Hazardous Materials*, **172**, 353–362.

Shen, Y.-H. (2002) Removal of phenol from water by adsorption–occulation using organobentonite. *Water Research*, **36**, 1107–1114.

Uslu, Y.O., İşçi, S., and Ece, Ö.I. (2009) Modification of montmorillonite with cationic surfactant and application in electrochemical determination of 4-chlorophenol. *Materials Characterization*, **60**, 432–436.

Vuković, Z., Milutinović-Nikolić, A., Rožić, Lj., Rosić, A., Nedić, Z., and Jovanović, D. (2006) The influence of acid treatment on the composition of bentonite. *Clays and Clay Minerals*, **54**, 697–702.

Wang, C.C., Juang, L.C., Lee, C.K., Hsu, T.C., Lee, J.F., and Chao, H.P. (2004) Effect of exchanged surfactant cations on the pore structure and adsorption characteristics of montmorillonite. *Journal of Colloid and Interface Science*, **280**, 27–35.

Webb, P.A. and Orr, C. (1997) *Analytical methods in fine particle technology*. Micromeritics Instrument Corporation, Norcross, GA, USA.

Yang, H., Zheng, X., Huang, W., and Wu, K. (2008) Modication of montmorillonite with cationic surfactant and application in electrochemical determination of 4-chlorophenol. *Colloids and Surfaces B*, **65**, 281–284.

(*Received 7 October 2011; revised 26 April 2012; Ms. 622; A.E. F. Bergaya*)